Copyright © 2009 by ABCM

FRICTION LOSSES AT THE ENTRANCE OF A TUBE AND IN ABRUPT CONTRACTION FOR POWER-LAW AND BINGHAM FLUIDS

Sergio L. D. Kfuri, kfuri@ct.ufes.br
Johnny Q. Silva, johnny@ct.ufes.br
Edson J. Soares, edson@ct.ufes.br
LFTC-Department of Mechanical Engineering, Universidade Federal do Espirito Santo, Avenida Fernando Ferrari, 514, Goiabeiras, 29075-910, ES, Brazil

Roney L. Thompson, rthompson@mec.uff.br
LFTC-LMTA, Department of Mechanical Engineering (PGMEC), Universidade Federal Fluminense, Rua Passo da Patria 156, 24210-240, Niteroi, RJ, Brasil

Abstract. *Non-newtonian fluids are widely used in the petroleum industry and there are a huge class of these materials that can be modeled either as a power-law fluid, when the material exhibits pseudo-plastic behavior, or as a Bingham fluid, when the material possesses an yield stress. Pressure losses in piping systems result from a variety of sources that can be roughly divided into the wall friction, change in the flow direction, and change in the cross section of the duct. Here we use the commercial software Polyflow to measure the friction losses in two situations very common in pipe systems: the abrupt contraction and the entrance of a tube where the flow is not fully-developed. Two kinds of non-Newtonian materials are tested, a power-law fluid and a Bingham material, are compared with the Newtonian result. The main objective is investigate how the power-law index and the yield stress (through the Bingham number) influence these pressure losses. For the entrance region, we have found that as n decreases, friction loss also decreases, therefore a pseudoplastic fluid has a lower friction factor than a Newtonian one. In the same geometry, an increase in the Bingham number decreases the friction factor. For the abrupt contraction geometry, a decrease of the power-law index or an increase of the dimensionless yield stress increases the friction losses.*

Keywords: *Friction losses, non-Newtonian material, entrance flow, contraction flow, finite element method*

1. INTRODUCTION

The importance of non-Newtonian materials is becoming more and more recognized in the petroleum industry. One of the reasons is due to the increasing necessity of determining more accurately certain procedures that have a traditional Newtonian calculation counterpart. It was not uncommon, in the past, to use Newtonian results as an approximation for non-Newtonian flows. Another reason is that non-Newtonian materials are more complex, exhibiting features that are not present in Newtonian fluids world such like pseudoplasticity, viscoplasticity, elasticity, thixotropy. These features can be used in the design of new apparatus and to conceive new methodologies to optimize standard processes. Therefore, in the recovery of oil, drilling mud removal, among other procedures, the use of a non-Newtonian fluid is widely used. But, perhaps, one of the most important applications is related to heavy oils with non-Newtonian behavior.

A very relevant problem to the petroleum industry is the calculation of pressure loss in fittings and components of piping system where non-Newtonian materials flow. The energy consumption of the piping system and pump selection needed are dependent on such analysis. Despite of this fact, there are few works in the literature that investigate non-Newtonian pressure loss. Most of these works are experimental investigations. In this case, a change on the material is given by a change in a concentration of a set of particles that is added to a Newtonian solvent. With a new concentration, the material is characterized through its viscosity as a function of the shear rate. Generally these results are fitted by a chosen model (power-law, Sisko, Carreau) and the parameters of the model are used to understand the principles of friction loss in the fittings considered. The results are giving by a resistance coefficient parameter of the fitting, K, as a function of the Reynolds number. There are mainly two equations used to fit these curves. The one presented by Kittredge and Rowley (1957) where

$$K = A(Re)^{-B} \tag{1}$$

and the $two\ Ks$ method presented by Hooper (1981), where

$$K = \frac{K_1}{Re} + K_\infty \left(1 + \frac{1}{D}\right) \tag{2}$$

In general, for the the two Ks method, the first part proportional to the inverse of the Reynolds number, is related to the laminar regime, while the value K_∞ is constant level associated to the turbulent regime.

Turian et al. (1998) investigated the friction losses in some fittings with slurries of in a Newtonian fluid. They study not only laminar, but also turbulent flows with different concentration of two kinds of slurries: Titanium dioxide, Laterite,

and Gypsum. The model, used to fit the rheological viscosity curve was the Sisko model, given by

$$\eta = m\dot{\gamma}^{n-1} + \eta_\infty \tag{3}$$

where m and n are the consistency and exponent index of the power-law part and η_∞ is the asymptotic viscosity value for high values of the shear rate. The fittings investigated were: two kinds of valvulas gate, and globe; three elbows: with curvatures of 45^0, 90^0, and 180^0 degrees, a Venturi tube, and an abrupt expansion and contraction. They found that the two Ks method fits well the data. For the laminar regime, the values found for K_1 is independent of the diameter, while the values found for K_∞ are different, for different diameters.

The components tested by Bandyopadhyay and Das (2007), on their experimental apparatus, were orifices, globe and gate valves, and elbows of 45^0, 90^0, and 135^0 degrees. The tested fluid was a dilute solution of a sodium salt of carboxy methyl cellulose of high viscous grade. They fitted the viscosity function with a power-law equation. The main result of the article was to propose correlations for the different fittings as a function of the Reynolds number and a fitting parameter (such as the degree of the elbow curvature or the ratio of valve opening). The Reynolds number was calculated with an effective viscosity, μ_{eff}, given by

$$\mu_{eff} = m^* \left(\frac{8V}{D}\right)^{n^*-1} \tag{4}$$

The effective viscosity provides a product $fRe = 64$ independently of the material under investigation, in accordance to **?** and Soares et al. (2003). This happens because, in the fully developed region, $f = \frac{8\tau_w}{\rho V^2}$. The other important contribution was the experimental investigation of the influence of the diameter size on the friction losses in fittings when a non-Newtonian fluid is the main fluid of the hydraulic system. For this purpose, they have carried out their experiments with a tube of a small diameter, $d = 0.0127m$ and compared their results with other, from the literature, with tubes of regular diameter sizes.

The work of Polizelli et al. (2003) analyzes the laminar and turbulent non-Newtonian flows of aqueous solutions of sucrose and xanthan gum. Although the viscosity function was better fitted by a Hershell-Buckley model, the yield stress was too small and sometimes negative. Therefore, the power-law equation was chosen to fit the data. The tested fittings were elbows of 45^0, 90^0, and 180^0 and butterfly and plug valves. They used the two-K method for the different fittings finding a good agreement between predicted and experimental values.

Pinho et al. (2003) investigated the friction losses in sudden expansion $1 : 2.61$ for shear-thinning power-law fluids in the laminar regime. They propose a new way to calculate the Reynolds number for a best correlation of the results. They give also results for the size of the recirculation at the corner and the relative intensity of the stream function at the core of the recirculation.

2. PHYSICAL FORMULATION

2.1 Conservation equations

The velocity and pressure fields are defined by the governing equations that impose conservation of mass and momentum for an incompressible fluid, together with the appropriate boundary conditions. In the present work, the main hypothesis considering the flow conditions are

1. The fluid is incompressible.
2. Steady-state laminar regime.
3. The flow is axisymmetric.
4. Body forces are conservative.
5. Isothermal flow.

With these hypothesis, the conservation of mass is given by

$$\frac{1}{r}\frac{\partial}{\partial r}(rv) + \frac{\partial u}{\partial r} = 0, \tag{5}$$

while the conservation of momentum is given by

$$\rho\left(u\frac{\partial u}{\partial x} + v\frac{\partial u}{\partial r}\right) = \frac{1}{r}\frac{\partial}{\partial r}(rT_{xr}) + \frac{\partial}{\partial x}(T_{xx}) \tag{6}$$

$$\rho\left(u\frac{\partial v}{\partial x}+v\frac{\partial v}{\partial r}\right)=\frac{1}{r}\frac{\partial}{\partial r}(rT_{rr})-\frac{T_{\theta\theta}}{r}+\frac{\partial}{\partial x}(T_{rx})=0 \tag{7}$$

Where u and v are respectively the axial and radial components of the velocity field $\mathbf{u}$ and the quantities T_{xx}, T_{xr}, T_{rx}, T_{rr} and $T_{\theta\theta}$ are the components of the stress tensor $\mathbf{T}$.

2.2 Constitutive equations

In order to close the set of unknowns and equations given by Eqs. (5), (6), and (7), addition equations are needed. Generally they come from an assumption on the behavior of the material when it is subjected to a certain state of stress. This constitutive equation is, therefore, a relation between the stress tensor $\mathbf{T}$ and kinematics. In the present work, the material models are under a class called Generalized Newtonian Fluids (GNF) that obey the following constitutive equation

$$\mathbf{T}=-p\mathbf{1}+2\eta\mathbf{D} \tag{8}$$

where p is the mechanical pressure, η is a viscosity, and $\mathbf{D}\equiv 0.5\left(\nabla\mathbf{v}+\nabla^T\mathbf{v}\right)$ is the symmetric part of the velocity gradient. For a newtonian fluid, the viscosity $\eta=\mu$ is constant. For a GNF the viscosity is a function of the deformation rate $\dot{\gamma}$, a scalar that measures the intensity of the tensor $\dot{\boldsymbol{\gamma}}\equiv\nabla\mathbf{v}+\nabla^T\mathbf{v}=2\mathbf{D}$, given by

$$\dot{\gamma}=\sqrt{\frac{1}{2}\mathrm{tr}\left(\dot{\boldsymbol{\gamma}}^2\right)} \tag{9}$$

where tr indicates the trace operator of a tensor.

The two viscosity functions considered here are the power-law fluid and the Bingham material. As explained previously, the power-law constitutive equation is used when the operational flow conditions are in a range where viscosity decays (or goes up) with a constant slope in a log-log plot of viscosity as a function of the shear rate.

$$\eta=K\dot{\gamma}^{n-1} \tag{10}$$

where K is the consistency index, while n is the exponent index.

A Bingham viscosity function is used when the fluid has an yield stress, τ_0. Additionally when τ_0 is transposed, the fluid flows as a Newtonian one of viscosity μ_p.

$$\begin{cases}\eta=\frac{\tau_0}{\dot{\gamma}}+\mu_p & \text{if} \quad \tau\geq\tau_0\\ \eta\to\infty & \text{if} \quad \tau<\tau_0\end{cases} \tag{11}$$

2.3 General analysis

A simple conservation of mechanical energy, between an upstream position 1 and a downstream position 2, in a piping system under the hypothesis considered, leads to the well known equation

$$\frac{P_1}{\rho_1}+\alpha_1\frac{\bar{V}_1^2}{2}+gZ_1=\frac{P_2}{\rho_2}+\alpha_2\frac{\bar{V}_2^2}{2}+gZ_2+h_t, \tag{12}$$

where P_i, $\bar{V}_i$, Z_i are, respectively, the values of: the mechanical pressure, the mean velocity, and the height in the gravitational direction, at position i. The present analysis considers a modified pressure that incorporates the work done by gravitational forces. The coefficients α_i are related to non-uniformity of the velocity profile and are defined as

$$\alpha_i=\frac{1}{\bar{V}^3A}\int_A V^3dA. \tag{13}$$

For uniform velocity profiles, $\alpha=1$. In the case of a laminar fully-developed Newtonian flow, since the profile is quadratic, $\alpha=2$. The quantity h_t is the represents the total energy per unit of mass loss from point 1 to point 2.

The procedure followed in the present investigation is to split h_t into two parts: one part that considers the loss that would occur in a straight pipe in a fully-developed regime and a second part related to the change (associated to the fully-developed counterpart) in the flow profile caused by the accident considered.

Figure 1 depicts a scheme to illustrate the procedure and the calculation of a generic coefficient of local loss, K. Therefore, from Eq. (12) we have that

$$h_t=\sum_{j=1}^{nj}f_j\frac{L_j}{D_j}\frac{\bar{V}_j^2}{2}+\sum_{p=1}^{np}K_p\frac{\bar{V}_p^2}{2}=\frac{P_1-P_2}{\rho}+\alpha_1\frac{\bar{V}_1^2}{2}-\alpha_2\frac{\bar{V}_2^2}{2}, \tag{14}$$

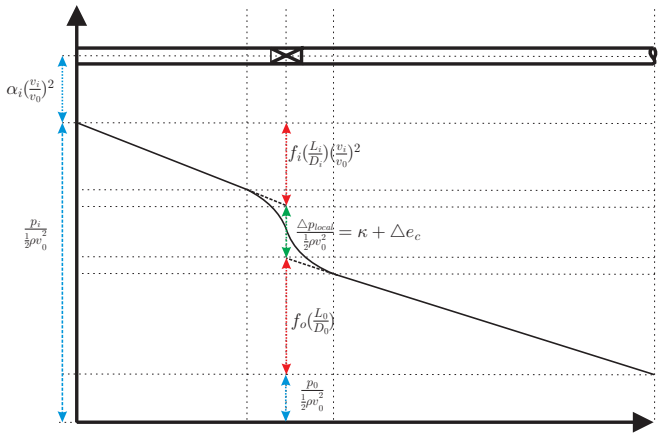

Figure 1. Dimensionless pressure loss in a hypothetic piping system. Calculation of of a generic coefficient of local loss, K.

where nj is the number of straight tubes and np is the number of accidents between positions 1 and 2. Quantities L_j, D_j, and $\bar{V}_j$ are the length, diameter and mean velocity of tube j, while $\bar{V}_p$ is a chosen characteristic mean velocity associated to accident p. Since we are investigating laminar losses, the friction factor associated to tube j is $f_j = \frac{64}{Re_j}$. K_p is local friction coefficient of accident p.

3. THE TWO PROBLEMS CONSIDERED

3.1 Entrance flow

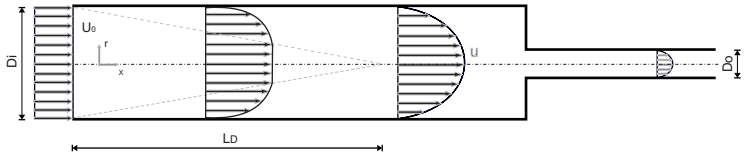

Figure 2. Dimensionless pressure loss in a hypothetic piping system. Calculation of of a generic coefficient of local loss, K.

The entrance flow considered in the present analysis is depicted on the left part of Fig.2. At the entrance the flow is considered uniform and then the profile evolves to a fully-developed configuration (before the contraction). The boundary conditions are

1. uniform profile at the inlet.
2. fully-developed flow at the outlet
3. no-slip condition at the wall
4. symmetry at the center of the tube

Position 1 is the inlet boundary, while position 2 is any position downstream where the flow has reached the fully-developed profile. The inlet velocity profile is consider uniform and, therefore $\alpha_1 = 1$. From Eq.(14) we see that $nj = np = 1$ and the mean velocity $\bar{V}$ is constant throughout the tube. The corresponding balance of energy equation is given by

$$h_{t(ent)} = \frac{64}{Re}\frac{L_{12}}{D}\frac{\bar{V}^2}{2} + K_e\frac{\bar{V}^2}{2} = \frac{P_1 - P_2}{\rho} + (1-\alpha_2)\frac{\bar{V}^2}{2}, \tag{15}$$

and so, the local friction coefficient of the entrance, K_e can be calculated as

$$K_e = \frac{P_1 - P_2}{\rho\frac{\bar{V}^2}{2}} + (1-\alpha_2) - \frac{64}{Re}\frac{L_{12}}{D}, \tag{16}$$

3.2 Abrupt contraction

Figure 2 shows the 4:1 abrupt contraction considered in the present analysis to determine the localized pressure loss. The boundary conditions for this problem are

1. fully-developed flow at the inlet and outlet.
2. no-slip condition at the wall.
3. symmetry at the centerline.

Position 1, in this case, is any position upstream the contraction where the flow still presents a fully-developed profile, while position 2 is any position downstream the contraction where the flow has reached the new fully-developed profile. From Eq.(14) we see that $nj = 2$ while $np = 1$. Since positions 1 and 2 correspond to fully-developed regions, $\alpha_1 = \alpha_2 = \alpha$. The corresponding balance of energy equation is given by

$$h_{t(cont)} = \frac{64}{Re_1}\frac{L_{1c}}{D_1}\frac{\bar{V}_1^2}{2} + \frac{64}{Re_2}\frac{L_{c2}}{D_2}\frac{\bar{V}_2^2}{2} + K_c\frac{\bar{V}_2^2}{2} = \frac{P_1 - P_2}{\rho} + \frac{\alpha}{2}\left(\bar{V}_1^2 - \bar{V}_2^2\right), \tag{17}$$

where K_c is the local friction coefficient of the contraction, based on the tube of smallest diameter. The quantities L_{1c} and L_{c2} are the lengths from position 1 to the contraction position and from the contraction position till position 2, respectively. The two mean velocities $\bar{V}_1$ and $\bar{V}_2$ are related by the continuity equation $\bar{V}_1 = \frac{1}{C_R^2}\bar{V}_2$, where C_R is the contraction ratio. Therefore, K_c is given by

$$K_c = \frac{P_1 - P_2}{\rho\frac{\bar{V}_2^2}{2}} + \alpha\left(\frac{1}{C_R^4} - 1\right) - \frac{64}{Re_2}\frac{L_{c2}}{D_2}\left(\frac{L_{1c}}{L_{c2}}\frac{1}{C_R^6} + 1\right), \tag{18}$$

Equation (18) reveals that as the contraction ratio increases, the total loss is dominated by the loss in the tube of smallest diameter.

4. NUMERICAL FORMULATION

4.1 Solution of the equation system by Galerkin / Finite Element Methods

The commercial software Polyflow 3.11.0 is used to solve the differential equations that govern the problem. They are solved in a coupled manner by the Galerkin/Finite Element Method. Biquadratic basis functions ϕ_j are used to represent the velocity and nodal coordinates, while linear discontinuous functions χ_j are employed to expand the pressure field. The velocity and pressure are represented in terms of appropriate basis functions

$$u = \sum_{j=1}^{n} U_j\phi_j \quad ; \quad v = \sum_{j=1}^{n} V_j\phi_j \quad ; \quad p = \sum_{j=1}^{m} P_j\chi_j \quad ; \tag{19}$$

The coefficients of the expansions are the unknown of the problem

$$\underline{c} = \left[\begin{array}{cccc} U_j & V_j & P_j \end{array}\right]^T$$

The corresponding weighted residuals of the Galerkin method related to conservation of momentum, mass and mesh generation are:

$$R_c^i = \int_{\bar{\Omega}}\left[\frac{1}{r}\frac{\partial}{\partial r}(rv) + \frac{\partial u}{\partial x}\right]\chi_i r||J||d\bar{\Omega} \tag{20}$$

$$\begin{aligned} R_{mx}^i &= \int_{\bar{\Omega}}\left[\frac{\partial\phi_i}{\partial x}T_{(xx)} + \frac{\partial\phi_i}{\partial r}T_{(xr)}\right]r||J||d\bar{\Omega} \\ &\quad - \int_{\bar{\Gamma}}\mathbf{e}_x\cdot(\mathbf{n}\cdot\mathbf{T})\phi_i r\frac{d\Gamma}{d\bar{\Gamma}}d\bar{\Gamma} \end{aligned} \tag{21}$$

$$\begin{aligned} R_{mr}^i &= \int_{\bar{\Omega}}\left[\frac{\partial\phi_i}{\partial x}T_{(xr)} + \frac{\partial\phi_i}{\partial r}T_{(rr)} + \frac{\phi}{r}T_{(\theta\theta)}\right]r||J||d\bar{\Omega} \\ &\quad - \int_{\bar{\Gamma}}\mathbf{e}_r\cdot(\mathbf{n}\cdot\mathbf{T})\phi_i r\frac{d\Gamma}{d\bar{\Gamma}}d\bar{\Gamma} \end{aligned} \tag{22}$$

4.2 Solution of the non-linear system of algebraic equation by Newton's Method

As indicated above, the system of partial differential equations, and boundary conditions is reduced to a set of simultaneous algebraic equations for the coefficients of the basis functions of all the fields. This set is non-linear and sparse. It is solved by Newton's method. The linear system of equations at each Newton iteration was solved using a frontal solver.

5. RESULTS

5.1 General

The velocity profiles, for different power-law exponents, are shown in Fig. 3. We can find a excellent agreement between them. We can also see (the expected result) that, as the fluid becomes more shear-thinning, the velocity profile becomes flatter. The analogous information for the visco-plastic material is shown in Fig. 4.

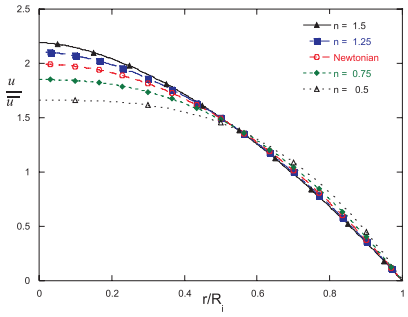

Figure 3. Local friction coefficient as a function of the Reynolds number for different power-law fluids wtih $n = 0.5$, 0.75, 1, 1.25 and 1.5.

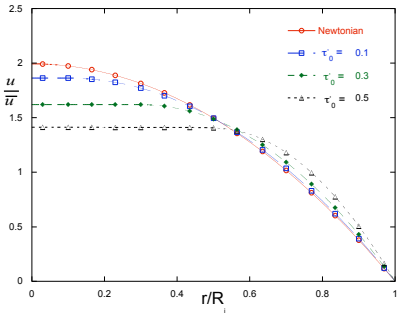

Figure 4. Local friction coefficient as a function of the Reynolds number for different Bingham materials wtih $\tau_0^{'} = 0$, 0.1, 0.3, and 0.5.

5.2 Entrance flow

5.2.1 Power-law

Figures 5 and 6 show the product of the friction factor times the Reynolds number, fRe as a function of the position along the entrance, for values of the Reynolds number $Re = 50$ and $Re = 1000$, respectively, for a power-law fluid for different levels of the exponent index, n.

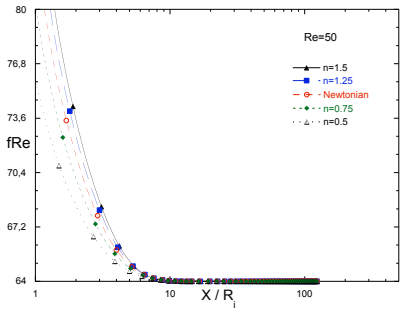

Figure 5. Local friction coefficient as a function of the Reynolds number for different power-law fluids wtih $n = 0.5$, 0.75, 1, 1.25 and 1.5.

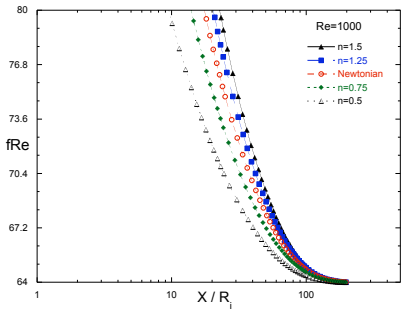

Figure 6. Local friction coefficient as a function of the Reynolds number for different power-law fluids wtih $n = 0.5$, 0.75, 1, 1.25 and 1.5.

We can see that, as the velocity profile approaches the fully-developed configuration, the product fRe tends to the value of 64, as expected. For the uniform profile, there is relative large dispersion of fRe which achieve higher values in the case of $Re = 1000$. The other worth noticing features of the curves is that they are more dispersed in the case

of the shear-thinning fluid curves, which shows the non-linearity feature of the problem. Even though, they behave monotonically.

5.2.2 Viscoplastic

Figure 7 shows the local friction coefficient K as a function of the Reynolds number for a Bingham material for different levels of the dimensionless yield-stress, $\tau_0^{'}$.

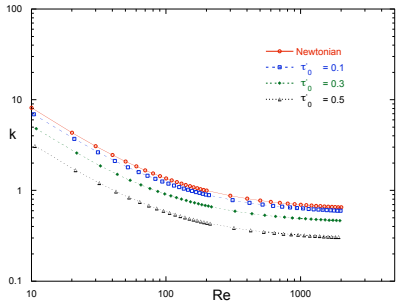

Figure 7. Local friction coefficient as a function of the Reynolds number for different Bingham materials wtih $\tau_0^{'} = 0$, 0.1, 0.3, and 0.5.

Figures 8 and 9 shows the product of the friction factor times the Reynolds number, fRe as a function of the position along the entrance, for values of the Reynolds number $Re = 50$ and $Re = 1000$, respectively, for a Bingham material for different levels of the dimensionless yield-stress, $\tau_0^{'}$.

As in the case of the power-law fluid, as the velocity profile approaches the fully-developed configuration, the product fRe tends to the value of 64. For the uniform profile, there is relative large dispersion of fRe which achieve higher values in the case of $Re = 1000$. As in other problems (Sousa et al., 2007) as the yield number increases, the viscoplastic material behaves, qualitatively, as a shear-thinning fluid.

5.3 Abrupt contraction

Figure 10 shows the local friction coefficient K as a function of the Reynolds number for a power-law material for different values of the exponent n. An interesting change in trends behavior happens after a critical value of Reynolds number. Before Re_c,

5.3.1 Viscoplastic

Figure 11 shows the local friction coefficient K as a function of the Reynolds number for a Bingham material for different levels of the dimensionless yield-stress, $\tau_0^{'}$.

6. DISCUSSION

The results obtained for the friction loss coefficient K are in accordance with some results in the literature (Pinho et al., 2003) and we are working on a function for this parameter that takes into account the rheology of the fluid also.

7. FINAL REMARKS

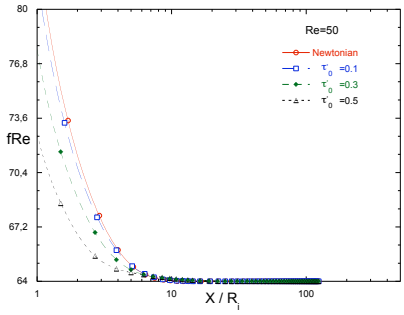

Figure 8. Local friction coefficient as a function of the Reynolds number for different Bingham materials wtih $\tau_0^{'} = 0$, 0.1, 0.3, and 0.5.

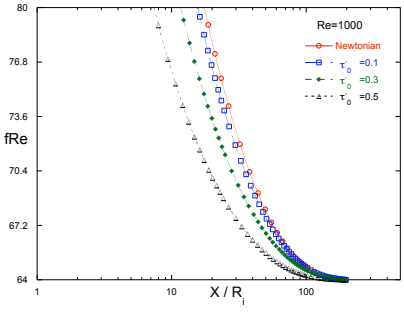

Figure 9. Local friction coefficient as a function of the Reynolds number for different Bingham materials wtih $\tau_0^{'} = 0$, 0.1, 0.3, and 0.5.

The present work have analyzed the local friction losses for two problems, the entrance flow from an uniform profile and a $4:1$ abrupt contraction, for power-law fluids and Bingham materials. The generalized Reynolds number employed was such that in the fully-developed region $fRe = 64$.

The main result have shown that the local friction coefficient K decays with the Reynolds number. There is still a need for fitting the data with the methods developed by Kittredge and Rowley (1957) and Hooper (1981).

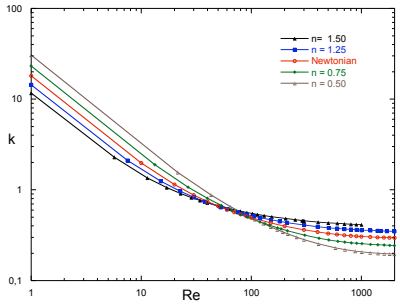

Figure 10. Local friction coefficient as a function of the Reynolds number for different power-law fluids wtih $n = 0.5$, 0.75, 1.0, 1.25, and 1.5.

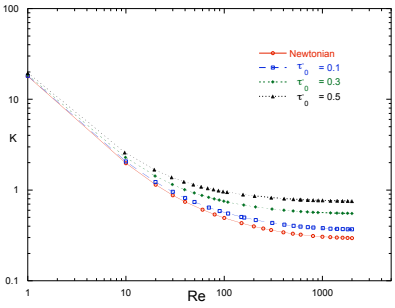

Figure 11. Local friction coefficient as a function of the Reynolds number for different Bingham materials wtih $\tau_0^{'} = 0$, 0.1, 0.3, and 0.5.

8. ACKNOWLEDGEMENTS

This research was funded by grants from PETROBRAS, ANP (Petroleum National Agency), and CNPq (the Brazilian Research Council).

9. REFERENCES

Copyright © 2009 by ABCM

Bandyopadhyay, T., Das, S., 2007. Non-newtonian pseudoplastic liquid flow through small piping components. J. Petroleum Sci. Eng. 55, 156–166.

Hooper, W., 1981. The two-k method predicts head losses in pipe fittings. Chem. Eng. 81, 96–100.

Kittredge, H., Rowley, R., 1957. Estimating friction loss coefficients. J. Fluid Mech. 81, 133–178.

Pinho, F. T., Oliveira, P. J., Miranda, J. P., 2003. Pressure losses in the laminar flow of shear-thinning power-law fluids across a sudden axisymmetric expansion. Int. J. Heat Fluid Flow 24, 747–761.

Polizelli, M., Menegalli, F., Telis, V., Telis-Romero, J., 2003. Friction losses in valves and fittings for power-law fluids. Braz. J. Chem. Eng. 20, 455–463.

Soares, E., Naccache, M., de Souza Mendes, P., 2003. Heat transfer to viscoplastic materials flowing axially through concentric annuli. Int. J. Heat Fluid Flow 24, 762–773.

Sousa, D., Soares, E., Queiroz, R., Thompson, R., 2007. Numerical investigation on gas-displacement of a shear-thinning liquid and a visco-plastic material in capillary tubes. J. Non-Newt. Fluid Mech. 144, 179–180.

Turian, R., Ma, T., Hsu, F., Sung, M., 1998. Flow of concentrated non-newtonian slurries: 2. friction losses in bends, fittings, valves and venturi meters. J. Multiphase Flow. 24, 243–269.

10. Responsibility notice

The author(s) is (are) the only responsible for the printed material included in this paper